Subject Independent Drunkenness Detection Using Pulse-Coupled Neural Network Segmentation of Thermal Infrared Facial Imagery

VICTOR-EMIL NEAGOE, SERBAN-VASILE CARATA
Faculty of Electronics, Telecommunications, and Information Technology
"Politehnica" University of Bucharest
Splaiul Independenței 313, Bucharest
ROMANIA
email: victor.neagoe@upb.ro

Abstract: - This paper proposes a new model of subject-independent drunkenness detection based on analysis of thermal infrared facial images. The method consists of the following processing stages: (a) thermal infrared image acquisition; (b) Pulse-Coupled Neural Network (PCNN) image segmentation; (c) feature selection using Principal Component Analysis (PCA) cascaded with Linear Discriminant Analysis (LDA); (d) Support Vector Machine (SVM) classification. We have built an experimental thermal infrared facial image database of 10 subjects (7 males and 3 females). The thermal images of each subject have been acquired both for sober condition and also for inebriation condition obtained after the person drank a specific amount of alcohol. Any thermal picture has been taken using a FLIR camera and it corresponds to the resolution of 160 x120 pixels in the wave range of 7.5-13 μm. The parameters of the PCNN have been optimized using a genetic algorithm. Using the proposed thermal image analysis cascade based on PCNN, we have obtained a drunkenness detection score of 97.5%, corresponding to an increase of 17.5% over the best score given by the considered benchmark method without PCNN segmentation.

Key-Words: - Drunkenness detection, thermal imagery, image segmentation, pulse-coupled neural network (PCNN), genetic algorithms

1 Introduction

All over the world, governments and private companies are putting biometric technology at the heart of ambitious projects, ranging from access control and company security to high-tech passports, ID cards, driving licenses, and company security. One of most important areas of biometric technology is face recognition using visual and/or thermal imagery [1], [2], [3], [4], [5], [6], [7]. Particularly, facial recognition technology could help trace terrorism suspects. A connected area with face recognition is emotion recognition by analyzing the facial expression; this belongs to the area of man-machine communication [8]. Face recognition based only on the visual spectrum has shown difficulties in performing consistently under uncontrolled operating conditions. Face recognition accuracy degrades quickly when the lighting is dim or when it does not uniformly illuminate the face [1], [4], [7]. Light reflected from human faces also varies depending on the skin color of people from different ethnic groups. The use of thermal infrared (IR) images can improve the performance of face recognition under uncontrolled illumination conditions [2], [3], [5]. Thermal IR spectrum comprising mid-wave IR (3-5μm) and long-wave IR (8-12μm) bands has been suggested as an alternative source of information for detection and recognition of faces [6]. Thermal IR sensors measure heat energy emitted, not reflected, from the objects. Hence thermal imaging has great advantages in face recognition [6], in low illumination conditions or even in total darkness, where visual face recognition techniques fail.

Road accidents are a global menace in every country [9], [10]. The Global status report on road safety 2013 compiled by the United Nations (UN) presents information on road safety from 182 countries, accounting for almost 99% of the world's population [9]. The report indicates that worldwide the total number of road traffic deaths remains unacceptably high at 1.24 million per year. Only 28 countries, covering 7% of the world's population, have comprehensive road safety laws on five key risk factors: drinking and driving, speeding, and failing to use motorcycle helmets, seat-belts, and child restraints [9]. The figures increase at an alarming rate every year. If no action is taken, the number of fatalities will increase to 2.4 million by 2030 [9]. A significant ratio of these accidents are

caused by drivers being intoxicated above the legal limit. *The research described here addresses this issue through analysis of the thermal infrared facial imagery*. *Drunkenness* is a challenging physiological condition to be investigated with applications to test driver (sober/drunk) condition [11]. However, most of the publications refer only to automotive anti-drunk driving systems, which use electrical signals from the heart or brain [12]. Koukiou and Anastassopoulus have recently published several papers having as aim drunkenness diagnose using processing of thermal infrared facial imagery [13], [14], [15], [16]. The success of this kind of approach is based on the fact that arteries and vessels on the face of a drunk person increase activity with the consumption of alcohol [16].

On the other side, there has been an increasing interest in using artificial neural networks (ANN) for image processing and pattern recognition [17], [18]. One of the most exciting neural network that recently has proven to be a viable method for image processing is Pulse-Coupled Neural Network (PCNN) [19], [20].The PCNN model is a biological inspired type of neural network, whose functions are found in the visual cortex of the cat [10] and some authors claimed that it can lead to a perfect image segmentation [21], [22], [23].

Within this paper we propose an original approach of drunkenness diagnose using a processing cascade of PCNN thermal infrared facial image segmentation followed by feature selection by Principal Component Analysis (PCA) – Linear Discrimant Analysis (LDA) and finally a Support Vector Machine (SVM) classifier. We have built an original database of thermal images for the sober/drunk subject condition (10 persons). The experimental results are given.

2 A New Thermal Image Analysis Algorithm for Drunkenness Diagnose

The proposed algorithm for inebriation diagnose has the following thermal image processing stages (Fig.1):

(i) Thermal infrared image acquisition
(ii) PCNN image segmentation
(iii) Loading of the PCNN segment pixels with corresponding grey levels
(iv) PCA
(v) LDA
(vi) SVM classifier

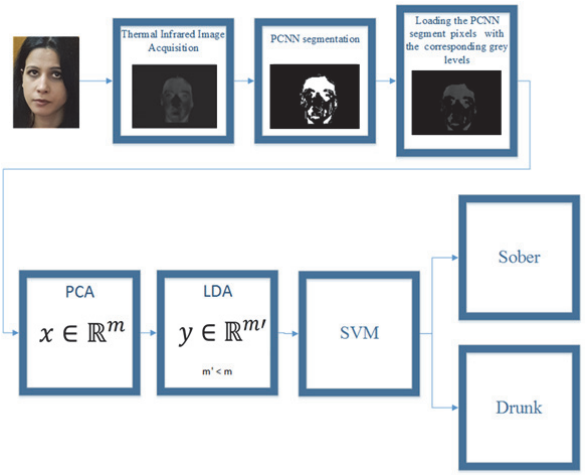

Fig. 1. Flowchart
of the drunkenness diagnose cascade.

The above mentioned processing stages are further presented in detail by selecting and grouping them in a few essential steps.

2.1 PCNN image segmentation

2.1.1 PCNN model

The Pulse-Coupled Neural Network (PCNN) model is a biological inspired type of neural network; its functions are found in the visual cortex of mammals [19], [20], [21]. It is a single layered, two-dimensional, laterally connected network of pulse-coupled neurons. There exists a one-to-one correspondence between the image pixels and network neurons. The PCNN equations are given below [19], [20], [21], [22], [23]

$$F_{ij}[n] = \exp(-\alpha_F) * F_{ij}[n-1] + V_F \sum_k \sum_l M_{ijkl} Y_{kl}[n-1] + S_{ij} \quad (1)$$

$$L_{ij}[n] = \exp(-\alpha_L) * L_{ij}[n-1] + V_L \sum_k \sum_l W_{ijkl} Y_{kl}[n-1] \quad (2)$$

$$U_{ij}[n] = F_{ij}[n]\left(1 + \beta L_{ij}[n]\right) \quad (3)$$

$$E_{ij}[n] = E_{ij}[n-1] \exp(-\alpha_E) + V_E Y_{ij}[n-1] \quad (4)$$

$$Y_{ij}[n] = \begin{cases} 1, & if\ U_{ij}[n] > E_{ij}[n] \\ 0, & otherwise \end{cases} \quad (5)$$

where α_F, α_L, and α_E are the time constants; V_F, V_L, and V_E are the magnitude adjustments; β is the linking strength of the PCNN. Each neuron is denoted with indices (i, j), and one of its neighboring neurons is denoted with indices (k, l). Feeding component $F_{ij}[n]$ is combined with linking component $L_{ij}[n]$ into neuron's internal activity

$U_{ij}[n]$. The neuron receives input signals via feeding synapse M_{ijkl}, and each neuron is connected to its neighbors such that the output signal of a neuron modulates the activity of its neighbors via linking synapse W_{ijkl}. The pulse is able to feed back to modulate the threshold $E_{ij}[n]$ via a leaky integrator, raising the threshold by magnitude V_E that decreases with time constant α_E. During iterations, when a neuron's internal activity $U_{ij}[n]$ exceeds its dynamic threshold $E_{ij}[n]$, a pulse is generated (firings).

2.1.2 PCNN-image segmentation

The input taken thermal images are processed according to the previously presented PCNN model. The extracted segments are composed by the pixels that fired at the moment of n-th iteration, namely those whose corresponding neurons outputs become "1" at this iteration according to equation (5).

We have used a genetic algorithm (GA) [24] to optimize the following seven parameters of the PCNN segmentation model: *the number of iterations n*; *the linking strength* β; *the link arrange representing the size of matrix M/W*; *the time constants* $\alpha_F=\alpha_L$ *and* α_E; *the magnitude adjustments* $V_F=V_L$ *and* V_E. The AG parameters are: *chromosome population; crossover rate; mutation rate; elite count; stop generation*. The fitness function for GA is the score of correct diagnose/classification of PCNN extracted segments in sober/drunk classes. As a result of PCNN segmentation, we obtain a set of white pixels belonging to the segments placed in a background of black pixels.

2.1.3 PCNN segment loading with corresponding grey levels

After extracting the pixels defining the segments, we load the PCNN segment pixels with corresponding grey levels.

2.2 Feature selection

2.2.1 Principal Component Analysis (PCA)

We have used Principal Component Analysis (PCA) as a first feature selection stage. Principal Component Analysis (PCA) is a statistical technique for optimal dimensionality reduction under least square sense that provides an orthogonal basis vector space to represent original data [18]. This technique searches for directions in the data that have largest variance and subsequently project the data onto it. We have applied PCA to transform the initially taken thermal image of S=pxq pixels corresponding to an S-dimensional space into a reduced m-dimensional space.

2.2.2 Linear Discriminant Analysis (LDA)

The second feature selection step corresponds to Linear Discriminant Analysis (LDA) [18]. By this technique we have performed a new dimensionality reduction from m to m', but opposite to PCA, by LDA we have taken into account the labels of the data belonging to the training set in order to increase the class separability.

2.3 SVM classification

We have chosen the Support Vector Machine (SVM) to classify the input PCNN grey level segments into two categories: *sober* and *drunk*. SVM classifies data with two class labels by determining a set of support vectors that belong to the set of training inputs that outline a hyperplane in the feature space. SVM provides a generic mechanism that fits the hyperplane surface to the training data using a kernel function. We have considered several kernel function (e.g. linear, polynomial, or radial basis function (RBF)) for the SVM during the training process that selects support vectors. For a parametric kernel such as RBF, we have also scanned a large range of values of its parameter (gamma /spread).

3 Experimental Results

3.1 Thermal image dataset for drunkenness diagnose

For experimental evaluation, we have built a thermal infrared facial image dataset for inebriation diagnose. Any picture has been taken using a FLIR ThermaCAM B2 camera and it corresponds to the resolution of 160 x120 pixels with the wave range of 7.5-13 μm. The thermal database contains 400 images, corresponding to J=10 subjects. The thermal images of each subject have been acquired both for sober condition and also for inebriation condition obtained after 30 minutes since the person drank 100 ml amount of whisky (with 40 degrees of alcohol). Each subject is represented by 40 images, 20 images for the *"sober"* condition and the other 20 for *"drunkenness"* condition. For each of the sober/drunk subject condition, we have considered half of the images for optimizing the parameters of the PCNN segmentation model using fitness function of the genetic algorithm and other half of the images are used for training and testing (validation) the SVM classifier for drunkenness diagnose.

We have chosen a *procedure of subject independent drunkenness recognition* using SVM classification that implies building datasets for each of the J=10 subjects. For the subject of index "i", we have built the dataset DSi, where i = (1,…,J); each set DSi is split into two sub-sets:

- LDSi – the learning dataset for the subject "i"; it is created using (J-1) pictures of the other persons from the dataset, and has a size of k x (J-1) x M pictures; k is the number of images for each of the M=2 drunkenness conditions (sober/drunk); for our database, we have considered k=10, leading to the number of 180 images for any LDSi
- TDSi – the test (validation) dataset for the subject "i" consisting of k x M pictures of the person "i", leading to the number of 20 images for any TDSi.

3.2 Performance evaluation

We have considered the following performances to evaluate the proposed model:

- TPi = true positives = *drunkenness* correctly detected for subject "i" (*drunk* images diagnosed as *drunk*)
- TNi = true negatives = *soberness* correctly detected for subject "i" (*sober* images diagnosed as *sober*)
- FPi = false positives = *sober* images of subject "i" diagnosed as *drunk*
- FNi = false negatives=*drunk* images for subject "i" diagnosed as *sober* (for i=1,…,10)
- Overal Accuracy:

$$OAi = 100 \times (TPi + TNi)/(TPi + TNi + FPi + FNi) \quad (6)$$

- False Alarm Rate:

$$FARi = 100 \times (FPi)/(TNi + FNi) \quad (7)$$

- Miss Alarm Rate:

$$MARi = 100 \times (FNi)/(TPi + FNi) \quad (8)$$

We have also computed the global performances indices OA, FAR, MAR, by averaging the indices defined by relations (6), (7), (8) over all the J=10 subjects.

3.3 Experimental performances

For the genetic algorithm used to optimize the PCNN parameters, we have chosen the following parameters:

- *population P=150*
- *crossover rate=0.8*
- *mutation rate=0.01*
- *elite count=0.05*
- *stop generation N=50.*

In Figs. 2, 3, 4, and 5 there are shown the processed image results of the proposed drunkenness diagnose cascade corresponding to 4 of 10 subjects.

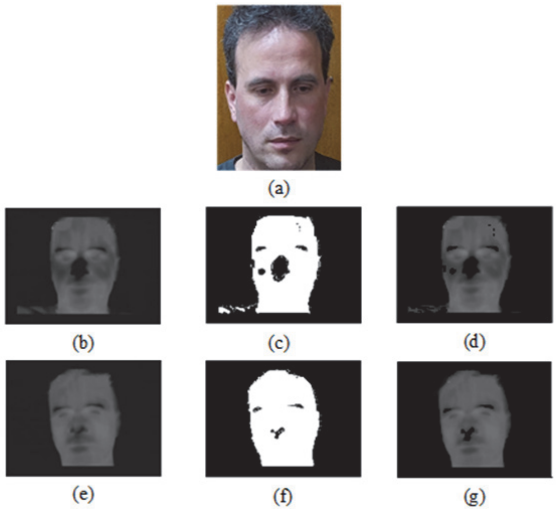

Fig. 2. Gabriel: (a) visible spectrum image; (b) input thermal infrared image, sober; (c) PCNN segmented picture (white corresponds to the segments), sober; (d) grey level loaded PCNN extracted segments, sober; (e) input thermal infrared image, drunk; (f) PCNN segmented picture (white corresponds to the segments), drunk; (g) grey level loaded PCNN extracted segments, drunk.

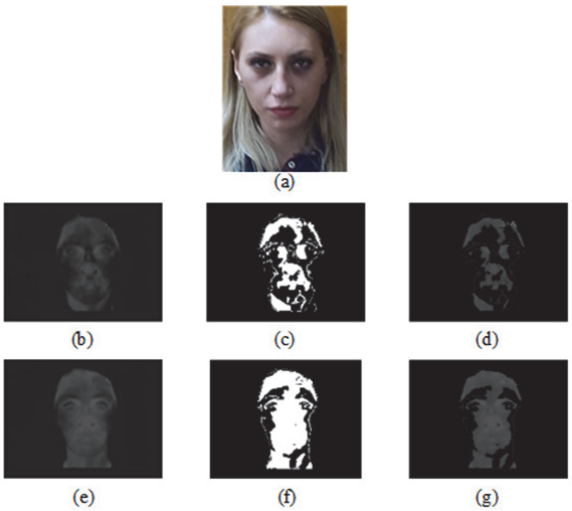

Fig. 3. Michaela: (a) visible spectrum image; (b) input thermal infrared image, sober; (c) PCNN segmented picture (white corresponds to the segments), sober; (d) grey level loaded PCNN extracted segments, sober; (e) input thermal infrared image, drunk; (f) PCNN segmented picture (white corresponds to the segments), drunk; (g) grey level loaded PCNN extracted segments, drunk.

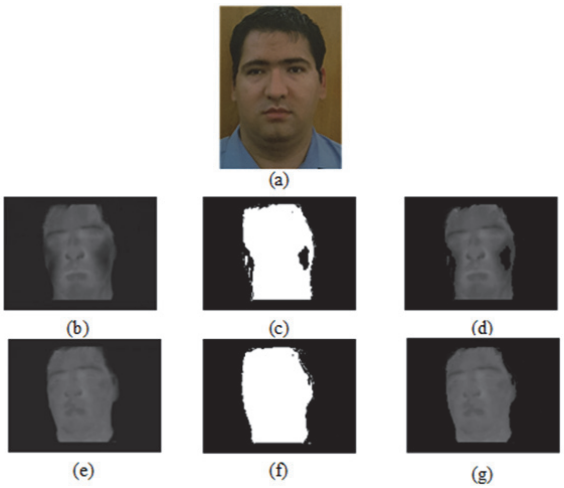

Fig. 4. Adrian: (a) visible spectrum image; (b) input thermal infrared image, sober; (c) PCNN segmented picture (white corresponds to the segments), sober; (d) grey level loaded PCNN extracted segments, sober; (e) input thermal infrared image, drunk; (f) PCNN segmented picture (white corresponds to the segments), drunk; (g) grey level loaded PCNN extracted segments, drunk.

Fig. 5. Cristina: (a) visible spectrum image; (b) input thermal infrared image, sober; (c) PCNN segmented picture (white corresponds to the segments), sober; (d) grey level loaded PCNN extracted segments, sober; (e) input thermal infrared image, drunk; (f) PCNN segmented picture (white corresponds to the segments), drunk; (g) grey level loaded PCNN extracted segments, drunk.

The final diagnose provided by SVM classifier must diagnose between the pictures grey level loaded PCNN extracted segments sober/drunk as shown in Figs. 6 and 7.

Fig. 6. Final processed pictures to be diagnosed for Gabriel: (a) grey level loaded PCNN extracted segments, sober; (b) grey level loaded PCNN extracted segments, drunk.

Fig. 7. Final processed pictures to be diagnosed for Michaela: (a) grey level loaded PCNN extracted segments, sober; (b) grey level loaded PCNN extracted segments, drunk.

For the PCA feature selection stage, we have chosen m=150 features; for the LDA feature selection, we have selected m'=1.

The performance evaluation of the experimental results for subject independent drunkenness diagnose using the proposed PCNN segmentation-based processing cascade are given in Table 1.

For comparison, we have shown in Table 2 the results of the processing cascade without PCNN segmentation stage (by processing the whole thermal image).

In Tables 3 and 4 there are shown the individual and global confusion matrices obtained by experimenting the proposed method.

Table 1. Performance evaluation for subject independent drunkenness diagnose using the proposed PCNN segmentation-based processing cascade (m PCA=150; m' LDA=1)

Kernel and parameters of SVM classifier	Link arrange (size of M/W matrix)	n (number of PCNN iterations)	$V_L = V_F$	V_E	$\alpha_L = \alpha_F$	α_E	β	OA (%)	MAR (%)	FAR (%)
Linear	4	3	0.1	0.31	2.8	16.6	0.4	97.5	1	4
Polynomial of 2 degree	4	3	0.1	0.31	2.8	16.6	0.4	97.5	1	4
Polynomial of 3 degree	4	3	0.1	0.31	2.8	16.6	0.4	97.5	1	4
Polynomial of 4 degree	4	3	0.1	0.31	2.8	16.6	0.4	97.5	1	4
Polynomial of 5 degree	4	3	0.1	0.31	2.8	16.6	0.4	97.5	1	4
RBF sigma=0.571	6	5	0.28	0.63	36.03	2.05	3.62	97.5	1	4
RBF sigma=1	6	5	0.28	0.63	36.03	2.05	3.62	97.5	1	4

Table 2. Performance evaluation for subject independent drunkenness diagnose using the processing cascade without PCNN segmentation stage (by processing the whole thermal image) (m PCA=150; m' LDA=1)

Kernel and parameters of SVM classifier	**OA (%)**	**MAR (%)**	**FAR (%)**
Linear	77.5	24%	14%
Polynomial of 2 degree	76.5	24%	16%
Polynomial of 3 degree	78	20%	17%
Polynomial of 4 degree	76.5	16%	23%
Polynomial of 5 degree	80	8%	23%
RBF sigma=0.411	77	24%	0%
RBF sigma=1	77.5	24%	21%

Table 3. Confusion matrix of subject "i" for subject independent drunkenness diagnose using the proposed PCNN-based processing cascade (m PCA=150; m' LDA=1; as one can see from Table 1 the results do not depend on SVM type)

Subject index "i"	1		2		3		4		5	
Real state of drunkenness→ *Assigned state* ↓	sober	drunk	sober	drunk	sober	drunk	sober	drunk	sober	drunk
sober	100%	0%	100%	0%	100%	0%	90%	10%	100%	30%
drunk	0%	100%	0%	100%	0%	100%	10%	90%	0%	70%
Subject index "i"	6		7		8		9		10	
Real state of drunkenness → *Assigned state* ↓	sober	drunk	sober	drunk	sober	drunk	sober	drunk	sober	drunk
sober	100%	0%	100%	0%	100%	0%	100%	0%	100%	0%
drunk	0%	100%	0%	100%	0%	100%	0%	100%	0%	100%

Table 4. Global confusion matrix for subject independent drunkenness diagnose using the proposed PCNN segmentation-based processing cascade (m PCA=150; m' LDA=1; as one can see from Table 1 the results do not depend on SVM type)

Real state of drunkenness → *Assigned state* ↓	sober	drunk
sober	99%	4%
drunk	1%	96%

4 Conclusion

The proposed new thermal image analysis algorithm for drunkenness diagnose has as a main novelty element the application of PCNN model for thermal image segmentation in the image processing cascade. It also uses several modern signal processing tools as Fisher cascade of PCA-LDA steps for feature selection and a genetic algorithm to optimize the parameters for the PCNN model.

We have built an original drunkenness detection thermal image database of 400 images corresponding to 10 subjects.

We have performed a detailed performance evaluation taking into account the overall accuracy (OA), missing alarm rate (MAR), false alarm rate (FAR) and confusion matrices. The experimental results confirm the proposed method; they do not depend on the type and parameters of the SVM classifier. The proposed method of thermal image analysis cascade for inebriation detection based on PCNN leads to very good performances as OA of 97.5% and MAR of 1%. The above scores are far better than the best ones obtained by the reference method using thermal imagery analysis without PCNN segmentation, namely OA of 80% and MAR of 8%.

References:

[1] Y. Adini, Y. Moses, and S. Ullman, Face recognition: The problem of compensating for changes in illumination direction, *IEEE Trans. on Pattern Analysis and Machine Intelligence*, Vol. 19, No. 7, July 1997, pp. 721-732.

[2] D.A. Socolinsky and A. Selinger, A Comparative Analysis of Face Recognition Performance with Visible and Thermal Infrared Imagery, *Proc. 16th Int'l Conf. Pattern Recognition*, Vol. 4, pp. 217-222, 2002.

[3] D.A. Socolinsky, A. Selinger, and J.D. Neuheisel, Face recognition with visible and thermal infrared imagery, *Computer Vision and Image Understanding*, Vol. 91, pp. 72-114, 2003.

[4] J. Heo, S.G. Kong, B.R. Abidi, and M.A. Abidi, Fusion of Visual and Thermal Signatures with Eyeglass Removal for Robust Face Recognition, *IEEE Workshop on ObjectTracking and Classification Beyond the Visible Spectrum in conjunction with CVPR 2004*, July 2004, Washington DC, pp. 94-99.

[5] P. Buddharaju, I.T. Pavlidis, P. Tsiamyrtzis, M. Bazakos, Physiology-Based Face Recognition in the Thermal Infrared Spectrum, *IEEE Trans. on Pattern Analysis and Machine Intelligence*, Vol. 29, No. 4, April 2007, pp. 613-626.

[6] V.E. Neagoe, A. Mugioiu and C. Tudoran, Concurrent Self-Organizing Maps for Multispectral Facial Image Recognition, *Proc. of the 2007 IEEE Symposium on Computational Intelligence in Image and Signal Processing (CIISP 2007)*, April 1-5, 2007, Honolulu, Hawaii, USA, pp. 330-335, ISBN:1-4244-0707-9.

[7] V.E. Neagoe, A. Ropot, and A. Mugioiu, Real Time Face Recognition Using Decision Fusion of Neural Classifiers in the Visible and Thermal Infrared Spectrum, *Proc. of the 2007 IEEE International Conference on Advanced Video and Signal based Surveillance (AVSS 2007)*, London (United Kingdom), 5-7 September 2007, pp. 1-6, ISBN:978-1-4244-1696-7.

[8] V.E. Neagoe, A.P. Barar, N. Sebe, P. Robitu, A Deep Learning Approach for Subject Independent Emotion Recognition from Facial Expressions, *Recent Advances in Image, Audio, and Signal Processing, Proc. 1st International Conference on Image Processing and Pattern Recognition (IPPR13)*, Budapest (Hungary), Dec. 10-12, 2013, pp. 93-98, ISBN: 978-960-474-350-6, ISSN:1790-5117.

[9] UN, *Road Safety report, 2013*. [Online]. Available: http://www.un.org/ar/roadsafety/pdf/roadsafetyreport.pdf.

[10] D. Isa, G.C. Chieh, R. Arelhi, Abnormal Driver Behavior Detection Using Parallel CPU and GPU Algorithm through Facial Expression, Thermal Imaging and Heart Rate Data Fusion, *Proc. International Journal of Engineering and Innovative Technology (IJEIT)*, Vol 2, Issue 3, September 2012, pp. 53-64, ISSN: 2277-3754.

[11] B. Hunicka, H. Laurell, and H. Bergman, Psychosocial Characteristics of Drunk Drivers Assessed by Addiction Severity Index, Prediction of Relapse, *Scandinavian Journal of Public Health*, February, Vol. 38, No. 1, 2010, pp.71–77.

[12] Y.C. Wu, Y.Q. Xia, P. Xie, and X.W. Ji, (2009) The Design of an Automotive Anti-Drunk Driving System to Guarantee the Uniqueness of Driver, *Proc. International Conference on Information Engineering and Computer Science (ICIECS 2009)*, December 2009, pp.1–4.

[13] G. Koukiou and V. Anastassopoulos, Drunk Person Identification Using Thermal Infrared Images, *Int. J. Electronic Security and Digital Forensics*, Vol. 4, No. 4, 2012, pp. 229-243.

[14] G. Koukiou and V. Anastassopoulos, Face Locations Suitable Drunk Persons Identification, *2013 International Workshop on Biometrics and Forensics (IWBF)*, Lisbon, 4-5 April 2013, pp. 1-4, ISBN 978-1-4673-4987-1.

[15] G. Koukiou and V. Anastassopoulos, Eye Temperature Distribution in Drunk Persons using Thermal Imagery, *Proc. 2013 International Conference of the Biometrics Special Interest Group (BIOSIG)*, Darmstadt, 5-6 Sept. 2013, pp. 233-240.

[16] G. Koukiou and V. Anastassopoulos, Neural Networks for Identifying Drunk Persons using Thermal Infrared Imagery, *Forensic Science International*, Vol. 252, July 2015, pp. 69–76.

[17] M.E.-Petersena, D. de Ridderb, H. Handelsc, Image processing with neural networks—a review, *Pattern Recognition*, Vol. 35, 2002, pp. 2279–2301.

[18] M. Bishop, *Pattern Recognition and Machine Learning*, Springer, New York, 2006.

[19] Y. Ma, K. Zhan, Z. Wang, *Applications of Pulse-Coupled Neural Networks*, Springer, Heidelberg-New York, 2010.

[20] T. Lindblad, J.M. Kinser, *Image Processing using Pulse-Coupled Neural Networks*, Springer, Berlin, 2005.

[21] G. Kuntimad and H.S. Ranganath, Perfect Image Segmentation Using Pulse Coupled Neural Networks; *IEEE Transactions on Neural Networks*, Vol. 10, May 1999, No. 3, pp. 591 – 598.

[22] V.E. Neagoe, S.V. Carata, A.D. Ciotec, Automatic Target Recognition in SAR Imagery using Pulse-Coupled Neural Network Segmentation Cascaded with Virtual Training Data Generation CSOM-based Classifier, 2015 *IEEE International Geoscience and Remote Sensing Symposium Proceedings (IGARSS 2015)*, Milano, Italy, July 26-31, 2015, pp. 3274-3277.

[23] S. V. Carata, V.E. Neagoe, An Innovative Pulse-Coupled Neural Network Approach to Image Segmentation, *Proceedings of 6th European Conference on Computer Science (ECCS"15)*, Rome, Italy, November 7-9 2015, pp. 137-141.

[24] R.L. Haupt, S.E. Haupt, *Practical Genetic Algorithms*, (2nd Ed.), Wiley, New York, 2004.